Photoemission intensities at the 3p threshold resonance of NiO and Ni

M. R. Thuler, R. L. Benbow, and Z. Hurych
Physics Department, Northern Illinois University, DeKalb, Illinois 60115
(Received 28 April 1982; revised manuscript received 30 July 1982)

We report photoemission spectra and intensity profiles of the $3d$ emission and the resonant valence-band satellites in NiO and Ni. Ni in Ni metal is in a $3d^9$ configuration, but Ni in NiO is in a $3d^8$ configuration. NiO gives an opportunity to study the effect of a larger number of holes in the d configuration: For NiO we find a very strong resonant satellite at 9.2 eV and a weak satellite at $\sim$22 eV below the main $3d$ peak. The intensity of the 9.2-eV satellite is about twice that of the 6.2-eV satellite in Ni, which reflects the increased number of empty $3d$ states of NiO as compared with Ni. The intensity profile of the main $3d$ emission in NiO shows a strong (30%) dip at the resonance threshold, the energy of which corresponds to the main absorption threshold as measured with the constant-final-energy spectroscopy technique and to the binding energy of the $3p$ core levels as determined by x-ray photoelectron spectroscopy. Our interpretation is incomplete because of the clouded theoretical picture of NiO, but the results for Ni and NiO agree qualitatively with recent calculations indicating that similar processes are involved in both cases. The strong increase of 3 eV in the satellite-main line separation energy could be due to the strong localization of the $3d$ electrons in NiO, which should lead to an increase in the effective Coulomb interaction.

I. INTRODUCTION

Resonant photoemission has attracted considerable interest since it was first observed on Ni.[1] Resonant satellites have now been found in numerous elements[2–5] and compounds.[4,6–8] The strong intensity enhancement at resonance is due to the interference of two excitation channels leading to the same final state. One channel involves the excitation of a core-level electron followed by a coherent (Auger-type) decay leaving two more or less correlated holes on one site. The same final state can be obtained by a shakeup process, as schematically shown in Fig. 1. With respect to the $3d$-band satellites, Cu and Ni represent two qualitatively different systems.

In Cu both channels must involve states of the $n=4$ shell ($4s,p,d$) because of the $3d^{10}$ initial-state configuration. At resonance, sharp satellites are observed showing typical multiplet structure of a $3d^8$ final-state configuration.[9] Important parameters such as the effective Coulomb interaction between the two holes can be readily obtained.[4] Far from resonance the intensity gradually vanishes because of the weaker $3d$-$4s,p$ interaction.[9]

In Ni, however, the proposed satellite[10] consists of an intra-d-subshell transition. It has a higher excitation probability because of the stronger intra-d-band interactions and, consequently, the satellite shows considerable intensity far from resonance [e.g., at x-ray photelectron spectroscopy (XPS) energies]. At the resonance threshold, a $3p$-$3d$ transition followed by a $3p\,3d\,3d$ super Coster-Kronig (sCK) decay can lead to a strong enhancement of the satellite state because of the high density of empty $3d$ states just above the Fermi level. Indeed, at resonance the Ni satellite at 6.2 eV from the $3d$ maximum is the most intense example studied so far. For Pd, which has a much lower $4d$ hole concentration, the satellite is considerably weaker.[5]

In order to investigate a system far removed from Cu and also very different from Ni metal, we therefore decided to measure the resonant behavior of NiO. For a $3d^8$ initial state [t_{2g} (Ref. 6), e_g (Ref. 2)] there are two empty d states per Ni atom as compared to less than one d hole in Ni.[11] If indeed the resonance in the open $3d$-subshell elements is due to a $3p \rightarrow 3d$ transition (as compared to possible $3p \rightarrow 4s,p,d$ transitions), we expect the strength of the resonant enhancement to reflect the number of empty d states. Furthermore, it is interesting to see the effects of changing the d occupancy on both the multiplet splitting and the energy separation of the satellites, since they are believed to be mainly atomic in origin.[6,7] The interpretation of the resonance in NiO reveals the necessity of a better description of

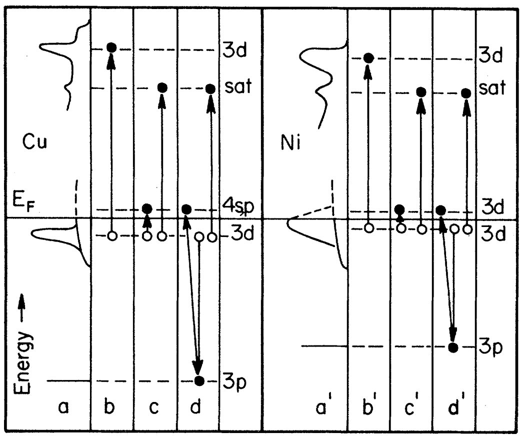

FIG. 1. Schematic representation of the photoionization processes expected for Cu ($3d^{10}$, left side) and Ni ($3d^{n<10}$, right side). *a* shows the occupied density of initial states below E_F and a sketch of a valence-band spectrum as measured with photoemission at resonance above E_F. *b*, continuum $3d$ photoemission leading to a bandlike final state (dispersive). *c*, continuum $3d$ photoemission accompanied with a $3d \rightarrow 4sp$ shakeup transition. The localized (nondispersive) final state shows multiplet splitting of an atomic $3d^8$ configuration and is screened by the $4sp$ electron in a possibly excitonic state. *d*, resonant channel consisting of a $3p \rightarrow 4sp$ threshold absorption followed by a $3p\,3d\,3d$ super Coster-Kronig decay leading to the same final state as in *c*. *a'*,*b'*,*c'*, and *d'* depict analogous processes for Ni. The only significant difference is the $3d$ character of the photoabsorption and shakeup final state. *b'* describes a bandlike final state while *c'* gives a two-hole state where the two holes are localized on one atom and interact with the effective Coulomb interaction (see Ref. 10).

the nature of the leading valence-band peaks, hitherto interpreted as crystal-field-split $3d^{n-1}$ multiplets in transition-metal compounds.

II. EXPERIMENTS

The experiments were made using synchrotron radiation from the electron storage ring Tantalus I at the University of Wisconsin. The photoelectron energy was measured with a double-stage cylindrical mirror analyzer in the angle-averaging mode. Its axis was normal to the incident light and in the polarization plane. The sample was in a p-polarization configuration with the polar angle θ_{inc} of the light being $\simeq 45°$ along a [100] azimuth. Total experimental resolution was $\Delta E \simeq 0.4$ eV and the working pressure was $p \lesssim 2\times 10^{-10}$ Torr.

NiO crystals were cleaved *in situ* showing mirror-like (100) planes. Charging up to ~ 5 V was observed in the NiO energy distribution curves (EDC). Figure 2 shows how energy positions could be determined by reducing the photon intensity drastically and extrapolating the energy positions to zero intensity. A second approach yielding the same value consisted in slightly heating the crystal to $T \lesssim 200\,°C$, therefore increasing the bulk conductivity. Higher temperatures lead to surface reduction,[12,13] which is readily observed, as photoemission in the energy gap appears. A Ni(100) single crystal was measured for comparison. The latter was cleaned by low-energy argon bombardment followed by annealing.

III. RESULTS AND DISCUSSION

Figure 3 shows the partial photoelectron yield spectra for Ni and NiO as determined by the low-energy constant-final-state energy spectroscopy (CFS) technique. In most cases this is equivalent[14] to a photon absorption measurement. The absorption experiments were made by Brown *et al.*[15] and are virtually identical. The CFS data shown in Fig. 3 are raw data not corrected for the light-intensity variation and a gradual decay of the stored beam current ($<2\%$). The photocurrent of a Au diode is shown for comparison. For Ni the half-height for the lower threshold is at 65.75 ± 0.1 eV (width ~ 1.2 eV). This agrees very well with the $3p_{3/2}$ binding energy as determined by XPS,[16] $E_b = 65.75$ eV. The

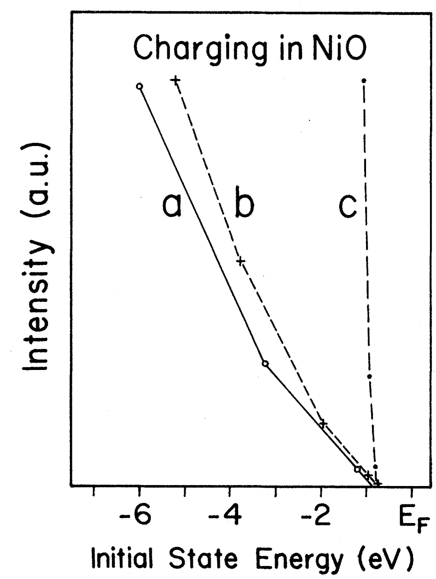

FIG. 2. Position of the leading edge (half-height) of the d-band peak as a function of light intensity due to charging of NiO. *a*, normal emission, p-polarized light, $h\nu = 22$ eV. *b*, normal emission, s-polarized light, $h\nu = 33$ eV. *c*, same as *b* but at an elevated temperature, $T \simeq 200\,°C$. The extrapolation to zero intensity gives $E_i \simeq 0.7$ eV for uncharged NiO.

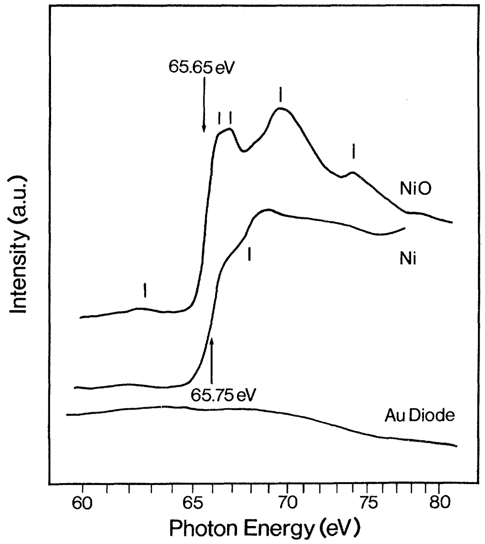

FIG. 3. Constant-final-state energy spectra for Ni ($E_f = 10$ eV) and NiO ($E_f = 2$ eV, $T \simeq 200\,^{\circ}$C). The photon-energy resolution was $\Delta E = 0.05$ and 0.07 eV, respectively. The increase at threshold amounted to 58% (Ni) and 43% (NiO) of the intensity below threshold. The lowest curve is a photoyield measurement for this monochromator as measured with a Au diode on a comparable scale. The numbers give the energy position of the half-height of the main threshold and the vertical lines give the position of additional structures in the absorption profiles as described in the text. (Note the nonlinear energy scale.)

second structure at ~2-eV higher binding energy is attributed to the excitation of the $3p_{1/2}$ core level. Published values of the spin-orbit (SO) splitting are $\Delta E_{so} = 1.4$ and 1.7 eV.[16] For Ni metal the final state of the photoabsorption is $3p^5 3d^{10}$. As the 3*d* band is full, the $3p^5 3d^{10}$ state shows only the spin-orbit splitting of the 3*p* core levels.

For NiO the initial state of the photoabsorption is $3p^6 3d^8$, and the final states expected close to the threshold are $3p^5 3d^9$ and $3p^5 3d^8 4s^1$. A recent study[17] on Cu dihalides ($3d^9$) suggests that the final states expected after 3*p* photoionization are $p^5 3d^n$ and $p^5 3d^{n+1}\underline{L}$. Here $\underline{L}$ means a hole in the ligand valence orbitals and the $n+1$ stems from the so-called ligand-to-metal 3*d* charge transfer. Therefore, for NiO ($3d^8$), the $3p^5 3d^8 4s^1$ final state might have a $3p^5 3d^9 \underline{L} 4s^1$ component. However, the energy of the $p^5 3d^9 \underline{L} 4s^1$ configuration is estimated to have a 6 eV to 10 eV higher excitation energy $[E(4s^1) + E(\mathrm{O}\,2p)$, see below] than the $3p^5 3d^9$ configuration that is reached at threshold. Thus the $3p^5 3d^9 \underline{L} 4s^1$ final state is not considered at threshold. This important assumption is also supported by extensive absorption measurements on transition-metal dihalides.[18] They show that the near-edge absorption structures are virtually independent of the halogens Br, Cl, and F but vary systematically with the occupation of the 3*d* subshell of Cr, Mn, Fe, Co, and Ni. This rich structure is therefore interpreted in NiO to be due to the multiplet interaction of the 3*p* hole with the empty 3*d* states in the photoabsorption final states $3p^5 3d^9$ and $3p^5 3d^8 4s^1$. The photoabsorption curve of NiO is shown in Fig. 3. The half-height of the main threshold for NiO occurs at $E_{\mathrm{NiO}} = 65.65 \pm 0.1$ eV (width ~0.9 eV). This is almost the same threshold energy as in Ni metal. As XPS measurements on NiO (Refs. 19 and 20) show little or no chemical shift in the 3*p* core-level binding energies with respect to the metal, it is tempting[21] to place the final state of the photoabsorption process at threshold close to the Fermi level E_F. Therefore, we assume that the first sharp feature is due to a $3p \rightarrow 3d$ transition. Multiplet splitting of the $3p^5 3d^9$ configuration can then account for most of its structure. Contrary to an early assignment[15] the very-low-intensity band observed below the main threshold is probably not part of the $3p^5 3d^9$ multiplet as it is not observed in absorption spectra of Ni atoms[22] which also mostly have a $3d^8$ ground-state electron configuration. The second strong maximum at $h\nu \simeq 70$ eV can then be due to the threshold for $3p \rightarrow 4s$ band electron transitions. The remaining weak structure at $h\nu \simeq 75$ eV has been attributed previously to band-structure effects.[15] The placement of the empty 4*s* level at approximately 3 eV above E_F agrees with an observed[23] 3.8-eV photoabsorption threshold (energy gap, for $3d^8 \rightarrow 3d^7 4s^1$ transitions) and our topmost photoemission peak (due to a $3d^7$ photoemission final state) at the inital-state energy $E_i = 1.4$ eV in the valence-band spectra of NiO. The fact that discrete $3d^8 \rightarrow 3d^{8*}$ absorption peaks[23] (the asterisk denotes an excited state) are observed below that threshold may indicate that empty 3*d* states (namely the empty localized minority-spin e_g states[23]) are available close to E_F. A similar interpretation can be applied to a recent electron-energy-loss study.[24] There the 3*p* core-level ionization loss for NiO was observed to have the same energy as for Ni metal. For NiO however, a second energy-loss peak was found with a 2.9-eV-higher loss energy. As electrons have properties of a "white-light" source[25] the simultaneous excitation of $3p \rightarrow 3d$ and $3p \rightarrow 4s$ transitions can explain the occurrence of two 3*p* core-level ionization loss peaks.

Figure 4 shows selected valence-band (VB) spectra of NiO taken at photon energies close to the resonance. Two sharp peaks at $E_i = 1.4$ and 3.0 eV are the leading structures in the VB. They show no (< 0.3 eV) dispersion in normal-emission experiments, as expected for localized final states. The

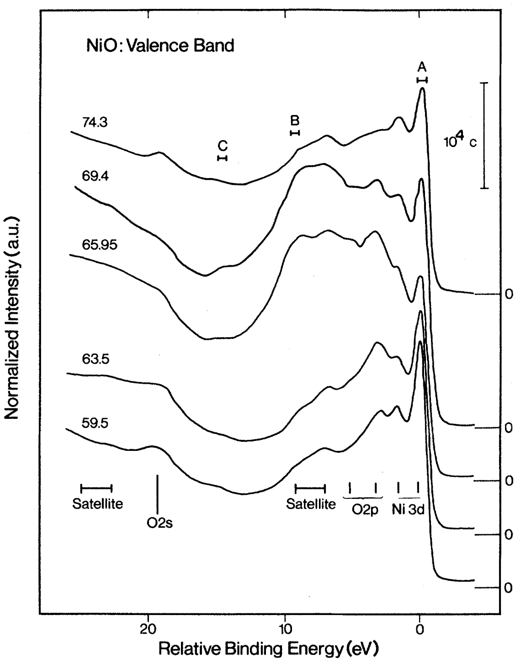

FIG. 4. Selected valence-band spectra of NiO at photon energies close to the resonance. The symbols and the letters A,B,C give the width and position of the regions, whose integrated intensity is plotted as a function of $h\nu$ in Fig. 6.

photon-energy dependence of their cross section clearly shows their d character as compared with the lower-lying structures which are identified as O $2p$—derived bands. This has led to the interpretation that the topmost structures are due to crystal-field—split $3d$ multiplets. In general, good agreement has been reported[26] between calculated and measured spectra of $3d^{n-1}$ multiplets (n = initial $3d$ occupation in an ionic model) for the transition-metal oxides and dichlorides of Mn, Fe, Co, and Ni. For NiO this implies that the main $3d$ emission is due to a $3d^7$ ionic final state. For the case of comparing our results with other measurements, all other peaks are given relative to the topmost peak (E_r). Angle-resolved normal-emission measurements show a strong dispersion of the O $2p$ bands within 1.6 eV $\lesssim E_r \lesssim 5.3$ eV.[27] The structures at $E_r = 1.6$, 3.2, and 5.2 eV are therefore attributed to critical points of the O $2p$ bands. The peak at $E_r = 19.2$ eV is the O $2s$ level. This behavior (nondispersive d states versus dispersive oxygen bands) agrees with the hybrid model proposed for the electronic structure of NiO.[23] Furthermore, the values for the critical points of the O $2p$ bands correspond well with those expected from a recent band-structure calculation (2.0, 3.0, and 5.2 eV).[28] The remaining structures at ~ 7 and ~ 9 eV are attributed to satellites. All energies given agree well with XPS measurements,[29] where, however, the O $2p$—derived bands are not observed (very weak cross section) and only one satellite is resolved at $E_r \simeq 7$–8 eV. At resonance ($h\nu \sim 67$ eV) a drastic enhancement is observed below the main $3d$ emission. Far above the resonance, the increasing $3d$ cross section and the decreasing O $2p$ cross section produce spectra similar to previously published XPS spectra.[29]

The location of the resonant satellites is best seen in a difference curve of EDC's above and below resonance. These are compared with Ni and NiO in Fig. 5. We find strong satellites at $\Delta E_{\rm Ni} = 6.2$ eV and at $\Delta E_{\rm NiO} = 9.2$ eV, and weaker ones at roughly 12.8 ± 1 eV and 22 ± 1 eV, respectively, from the main $3d$ maxima. Figure 5 illustrates the following: (i) With respect to the $3d$ main emission the resonance in NiO is considerably stronger than in Ni. This is expected because of the increased number of empty $3d$ holes per Ni atom and therefore supports the involvement of a local $3p \to 3d$ transition at resonance. (ii) Close to the resonance the intensity of the $3d$ emission is reduced in both Ni and NiO, thus giving a negative peak in the difference spectrum. This obscures possible structure on the low-binding-energy side of the resonant satellites. (iii) The increase (3 eV) in satellite-main line separation energy (ΔE) for NiO is probably the largest observed so far in resonance experiments on one atom in different environments. In the case of Ni and NiO this shift cannot be mainly caused by a shift in energy of the shakeup final state as in the case of Ga, GaP,[4] or in the case of Cu, Cu_2O,[8] because final states were

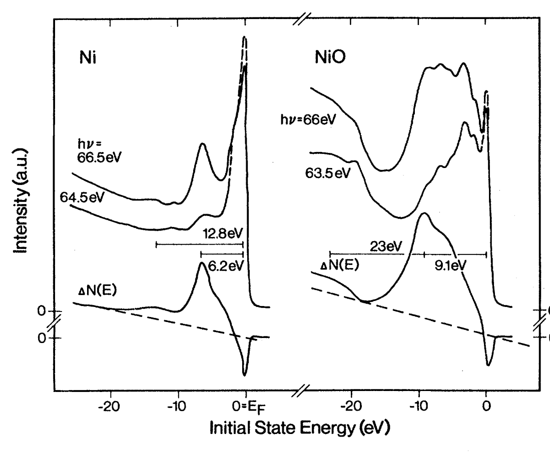

FIG. 5. Valence-band spectra and difference spectra of Ni and NiO for photon energies below and above the main absorption threshold. Note that the difference curves are shown with the same intensity scale being offset. Energy values given denote the separation of the maximum enhanced intensity from the leading $3d$ emission-peak position.

shown to be at E_F. The latter reports[4,8] also showed a decrease in the effective Coulomb interaction (which contains screening effects) for the $3d^8$ satellite final state in the insulating compounds. Therefore, the increase in ΔE_{NiO} is probably not due to screening effects. Because both Ni and NiO have empty d states, the model proposed by Penn[10] should apply in both materials. It predicts that an increase in the intra-atomic Coulomb interaction U moves the satellite state to higher binding energy and removes more weight from the main d-band emission. This could account for our results, at least qualitatively, if we assume that the strong localization[23] of the d states in going from Ni to NiO causes an increase in U. However, a more detailed comparison should also account for the (unresolved) multiplet splitting of the different localized final states involved for the satellite ($3d^7$ in NiO vs $3d^8$ in Ni metal).

An elegant method of examining the intensity distribution at the resonance is to measure constant initial-state-energy spectroscopy (CIS) curves. For NiO this is difficult because of the intensity-dependent charging. In this work series of EDC's were normalized to the electron-beam current in the storage ring and to accumulation time. CIS's were assembled from the series of EDC's by plotting the intensity of the corresponding energy region in each EDC. As the series of EDC's for NiO extended over more than one injected electron beam in the storage ring, a scaling factor had to be determined for each new beam to make adjoining portions of the CIS join smoothly. The scaling factor was determined by comparing the intensity of control measurements taken at a given photon energy. These yield variations are a common problem and are probably due to the exact position and the shape of the electron beam in the storage ring. We neglected the smooth variation of the monochromator transmission (see Fig. 3) because it does not introduce any sharp structure. The set of EDC's shown in Fig. 4 was normalized like this. The intensities of the indicated regions (A,B,C) are then plotted versus photon energy in Fig. 6. Apart from a generally decreasing intensity,[30] the distributions for the regions B and C resemble the CFS for NiO shown in Fig. 3. The threshold for the satellite resonance coincides with the CFS threshold. Using the same energy argument as before we see that the resonant satellite intensity is due to the decay of a $3p^5 3d^9$ state: $h\nu + 3p^6 3d^8 \rightarrow 3p^5 3d^9 \rightarrow 3p^6 3d^7 + e^-$. Therefore we do not believe that the satellite state contains a ligand-to-metal ($3d$) charge transfer ($3p^6 3d^8 \underline{L}$) in our photon-energy range $h\nu \leq 80$ eV. In addition, the charge-transfer final state could be identified with the direct emission from the ligand valence

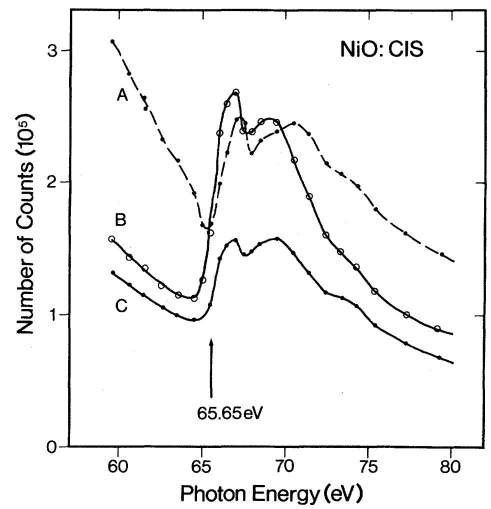

FIG. 6. Integrated intensities of the regions A,B,C indicated in Fig. 4 for NiO as a function of photon energy. Region A is centered on the $3d$ maximum, region B is centered 9.2 eV below that, where the resonant intensity increase is maximal, and region C lies ~ 5.5 eV below region B and therefore shows roughly the general enhancement due to core-hole decay electrons.

bands (O $2p$) which have a lower binding energy than the observed resonant satellites. Similar results were recently found for CuO.[8] Furthermore, a recently proposed[17] model to explain XPS results for Cu dihalides assumes that it is the main $3d$ emission rather than the satellite which should represent a charge-transfer final state. We therefore conclude that the valence-band satellite in NiO is not due to a ligand-to-metal ($3d$) charge transfer as proposed earlier.[29]

However, if the resonant enhancement identifies the NiO satellite with an atomiclike $3d^7$ final state, then the usual interpretation of the $3d$ main emission as a localized $3d^7$ multiplet must be questioned. The CIS for the topmost peak (Fig. 6, curve A) shows a large dip in intensity right at threshold, followed (possibly) by a weak enhancement. Clearly this behavior at resonance does not correspond to the expected increase for a $3d^7$ final state. Similar results have led Davis[31] to calculate the resonant intensities for a parametrized model[17] for the VB of transition metal compounds. In this model the amount of mixing in the initial two-hole states d^8 and $d^9 L^5$ determines whether the resonant enhancement is observed in the main lines or at higher binding energies. This depends on which of the VB features contains the most $3d^7 L^6$ characters as opposed to the nonresonant $3d^8 L^5$ and $3d^9 L^4$ final states. For reasonable parameters these calculations reproduce the resonant behavior observed in NiO quite well. However, it has yet to be established how well the nonresonant final states correspond to the rich structures in the direct VB emission (including dispersive bands) of different transition-metal compounds. Further work is therefore necessary to firmly establish any one of the interpretations given so far for the VB spectra of NiO.

CIS curves for Ni metal, similar to those for NiO, are shown in Fig. 7 and agree well with earlier results.[32] The observed dip in the 3d emission at threshold is roughly half as big as in NiO. Intensity profiles of the 3d emission have recently been calculated[33] for Ni and agree well with our results. This agreement includes the fact that the minimum of the 3d emission occurs at lower $h\nu$ than the maximum in the satellite emission for both NiO and Ni.

For Ni the same difference in the resonant behavior as for NiO is observed between the primary VB emission and the satellites. While the 6-eV satellite has previously been attributed to an atomiclike $3d^8$ configuration,[34] the primary emission was considered to represent a bandlike state where the two 3d holes are not localized on the same atom and do not interact. This corresponds with the fact that angle-resolved photoemission studies on Ni metal show dispersive bands, which allow a detailed comparison with band-structure calculations. A similar final-state description is not easily transferable to NiO because there the 3d states are rather localized.

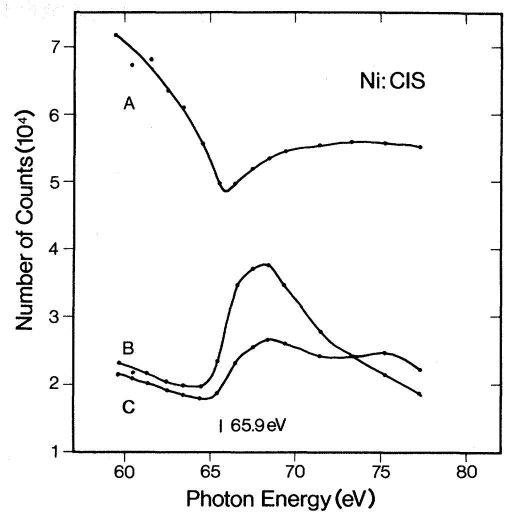

FIG. 7. Integrated intensities of 0.6-eV-wide regions as a function of $h\nu$ for Ni. The regions are centered: A at the 3d-band maximum, B at the resonant satellite, 6.1 eV below A, and C, 16.8 eV below A. The intensity from C then shows roughly the general background enhancement due to core-hole decay electrons. However, the weak maximum at $h\nu \sim 75$ eV is due to contributions from the direct nonresonant 3p 3d 3d Auger emission.

IV. SUMMARY

We have studied the resonant valence-band satellites in NiO and Ni using photemission with synchrotron radiation. At the Ni 3p photoabsorption threshold of NiO we observe a very strong enhancement of a satellite located approximately 9 eV below the leading 3d peak. The satellite at resonance is much stronger ($>2\times$) than in Ni metal, which is expected because of the increased number of empty 3d states available for the 3p excitations. For both materials an additional weak satellite with considerably large separation energy is found. Direct recombination effects produce a strong minimum in the 3d emission at the 3p threshold and show at most a weak enhancement at higher photon energies. For NiO, however, this may necessitate a reinterpretation of the VB spectra. The observed intensity profiles for both the satellites and the 3d primary emissions compare well with recent calculations. Our results therefore strongly support the proposed model for the resonance in systems with open 3d states. The large difference (3 eV) in the satellite separation energy between Ni and NiO may be due to an increased Coulomb interaction because of the strong localization of the 3d states in NiO.

ACKNOWLEDGMENTS

We thank Dr. Jean Brunner (Eidgenössische Technische Hochschule Zürich) for giving us a large NiO crystal, and Dr. Steven Kevan (Bell Laboratories) for lending us the Ni(100) crystal. The friendly assistance of the staff of the Synchrotron Radiation Center at Stoughton (supported by National Science Foundation Grant No. DMR-78-2188) is also gratefully acknowledged. This work was supported by National Science Foundation Grant No. DMR-81-08302.

[1] C. Guillot, Y. Ballu, J. Paigne, J. Lecante, K. P. Jain, P. Thiry, R. Pinchaux, Y. Petroff, and L. M. Falicov, Phys. Rev. Lett. 39, 1632 (1977).
[2] M. Iwan, F. J. Himpsel, and D. E. Eastman, Phys. Rev. Lett. 43, 1829 (1979).
[3] M. Iwan, E. E. Koch, T. C. Chiang, and F. J. Himpsel, Phys. Lett. 76A, 177 (1980).
[4] T. C. Chiang and D. E. Eastman, Phys. Rev. B 21, 5749 (1980).
[5] D. Chandesris, G. Krill, G. Maire, J. Lecante, and Y.

Petroff, Solid State Commun. 37, 187 (1981).

[6]D. Chandesris, C. Guillot, G. Chavin, J. Lecante, and Y. Petroff, Phys. Rev. Lett. 47, 1273 (1981).

[7]M. Iwan, E. E. Koch, T. C. Chiang, D. E. Eastman, and F. J. Himpsel, Solid State Commun. 34, 57 (1980).

[8]M. R. Thuler, R. L. Benbow, and Z. Hurych, Phys. Rev. B 26, 669 (1982).

[9]L. C. Davis and L. A. Feldkamp, Phys. Rev. Lett. 44, 673 (1980).

[10]D. R. Penn, Phys. Rev. Lett. 42, 921 (1979).

[11]The energy bands of Ni by C. S. Wang and J. Callaway, Phys. Rev. B 15, 298 (1977), which reproduce the measured magneton number of Ni ($0.56\mu_B$), were found to imply 0.9 empty 3*d* states by L. A. Feldkamp and L. C. Davis, Phys. Rev. B 22, 3644 (1980).

[12]K. Hirokawa, F. Honda, and M. Oku, J. Electron. Spectrosc. Relat. Phenom. 5, 333 (1975).

[13]J. Brunner and M. Thuler, Helv. Phys. Acta 50, 142 (1977).

[14]W. Gudat and C. Kunz, Phys. Rev. Lett. 29, 169 (1972).

[15]F. C. Brown, C. Gähwiller, and A. B. Kunz, Solid State Commun. 9, 487 (1971).

[16]See, e.g., table of core-level binding energies in *Photoemission in Solids II,* Vol. 2 of *Topics in Applied Physics,* edited by L. Ley and M. Cardona (Springer, Berlin, 1979).

[17]G. van der Laan, C. Westra, C. Haas, and G. A. Sawatzky, Phys. Rev. B 23, 4369 (1981), and references therein.

[18]S. Nakai, H. Nakamori, A. Tomita, K. Tsutsumi, H. Nakamura, and C. Sugiura, Phys. Rev. B 9, 1870 (1974).

[19]M. P. Hooker, J. T. Grant, and T. W. Haas, J. Vac. Sci. Technol. 13, 296 (1976).

[20]References on crystals must be carefully checked for charging effects. Charging does not, however, influence photoabsorption measurements.

[21]The assumption neglects relaxation effects due to the presence of an extra screening electron in threshold photoabsorption. Previous studies on CuO (Ref. 8) found a marked difference in 3*p* binding energy in threshold absorption experiments.

[22]R. Bruhn, B. Sonntag, and H. W. Wolff, J. Phys. B 12, 203 (1979).

[23]A large number of experimental results and a consistent model for the electronic structure of NiO is found in D. Adler and J. Feinleib, Phys. Rev. B 2, 3112 (1970), and references therein.

[24]C. Benndorf, B. Egert, G. Keller, H. Seidel, and F. Thieme, Surf. Sci. 80, 287 (1979).

[25]F. Gerken, J. Barth, K. L. I. Kobayashi, and C. Kunz, Solid State Commun. 35, 179 (1980).

[26]D. E. Eastman and J. L. Freehouf, Phys. Rev. Lett. 34, 395 (1975); T. Ishii, S. Kono, S. Suzuki, I. Nagakura, T. Sagawa, R. Kato, M. Watanabe, and S. Sato, Phys. Rev. B 12, 4320 (1975).

[27]M. R. Thuler, unpublished results.

[28]G. T. Surrat and A. B. Kunz, Solid State Commun. 23, 555 (1977).

[29]K. S. Kim, Chem. Phys. Lett. 26, 234 (1975) and references therein; *Photoemission in Solids II,* Ref. 16, Chap. 3.

[30]The CIS curves in Fig. 6 have not been corrected for the decreasing transmission of the cylindrical mirror analyzer. For CFS curves the transmission is of course constant, because the kinetic energy of the measured electrons is not changed.

[31]L. C. Davis, Phys. Rev. B 25, 2912 (1982).

[32]G. P. Williams, G. J. Lapeyre, J. Anderson, F. Cerrina, R. E. Dietz, and Y. Yaffet, Surf. Sci. 89, 606 (1979).

[33]L. C. Davis and L. A. Feldkamp, Phys. Rev. B 23, 6329 (1981).

[34]N. Martensson and B. Johannson, Phys. Rev. Lett. 45, 482 (1980).